New Phytologist

Tree height and hydraulic traits shape growth responses across droughts in a temperate broadleaf forest

Journal:	*New Phytologist*
Manuscript ID	Draft
Manuscript Type:	MS - Regular Manuscript
Date Submitted by the Author:	n/a
Complete List of Authors:	McGregor, Ian; Smithsonian Conservation Biology Institute, Conservation Ecology Center; North Carolina State University, Center for Geospatial Analytics Helcoski, Ryan; Smithsonian Conservation Biology Institute, Conservation Ecology Center Kunert, Norbert; Smithsonian Conservation Biology Institute, Conservation Ecology Center; Smithsonian Tropical Research Institute, Center for Tropical Forest Science Tepley, Alan; Smithsonian Conservation Biology Institute, Conservation Ecology Center Gonzalez-Akre, Erika; Smithsonian Conservation Biology Institute, Conservation Ecology Center Herrmann, Valentine; Smithsonian Conservation Biology Institute, Conservation Ecology Center Zailaa, Joseph; Smithsonian Conservation Biology Institute, Conservation Ecology Center; California State University Los Angeles, Biological Sciences Department Stovall, Atticus; Smithsonian Conservation Biology Institute, Conservation Ecology Center; University of Virginia, Department of Environmental Sciences; NASA Goddard Space Flight Center, Biospheric Sciences Bourg, Norman; Smithsonian Conservation Biology Institute, Conservation Ecology Center McShea, William; Smithsonian Conservation Biology Institute, Conservation Ecology Center Pederson, Neil; Harvard University, Harvard Forest Sack, Lawren; UCLA, Ecology and Evolutionary Biology; Anderson-Teixeira, Kristina; Smithsonian Conservation Biology Institute, Conservation Ecology Center; Smithsonian Tropical Research Institute, Center for Tropical Forest Science
Key Words:	annual growth, canopy position, drought, Forest Global Earth Observatory (ForestGEO), leaf hydraulic traits, temperate broadleaf deciduous forest, tree height, tree-ring

Title: Tree height and hydraulic traits shape growth responses across droughts in a temperate broadleaf forest

Authors: Ian R. McGregor[1,2], Ryan Helcoski[1], Norbert Kunert[1,3], Alan J. Tepley[1,4], Erika B. Gonzalez-Akre[1], Valentine Herrmann[1], Joseph Zailaa[1,5], Atticus E.L. Stovall[1,6,7], Norman A. Bourg[1], William J. McShea[1], Neil Pederson[8], Lawren Sack[9,10], Kristina J. Anderson-Teixeira[1,3]*

Author Affiliations:

1. Conservation Ecology Center; Smithsonian Conservation Biology Institute; National Zoological Park, Front Royal, VA 22630, USA
2. Center for Geospatial Analytics; North Carolina State University; Raleigh, NC 27607, USA
3. Center for Tropical Forest Science-Forest Global Earth Observatory; Smithsonian Tropical Research Institute; Panama, Republic of Panama
4. Canadian Forest Service, Northern Forestry Centre, Edmonton, Alberta, Canada
5. Biological Sciences Department; California State University; Los Angeles, CA 90032, USA
6. Department of Environmental Sciences, University of Virginia, Charlottesville, VA 22903, USA
7. NASA Goddard Space Flight Center; Greenbelt, MD 20771, USA
8. Harvard Forest, Petersham, MA 01366, USA
9. Department of Ecology and Evolutionary Biology; University of California, Los Angeles; Los Angeles, CA 90095, USA
10. Institute of the Environment and Sustainability; University of California, Los Angeles; Los Angeles, CA 90095, USA

*corresponding author: teixeirak@si.edu; +1 540 635 6546

Text	word count	other	n
Total word count (excluding summary, references and legends)	5,365	No. of figures	2 (both colour)
Summary	198	No. of Tables	5
Introduction	1,034	No of Supporting Information files	6
Materials and Methods	1,945		
Results	697		
Discussion	1467		
Acknowledgements	125		

Summary

- As climate change is driving increased drought frequency and severity in many forested regions around the world, mechanistic understanding of the factors conferring drought resistance in trees is increasingly important. The dendrochronological record provides a window through which we can understand how tree size and species' traits shape tree growth responses during droughts.
- We analyzed tree-ring records for twelve species that comprise 97% of the woody productivity of the 25.6-ha ForestGEO plot in an oak-hickory forest of northern Virginia (USA) to test hypotheses on how tree size, microenvironment characteristics, and species' traits shaped drought responses across the three strongest regional droughts over a 60-year period (1950 - 2009).
- Individual-level drought resistance decreased with tree height, which was the dominant size-related variable affecting drought response. Resistance was greater among species whose leaves lost turgor (wilted) at more negative water potentials, and whose leaves experienced less shrinkage upon desiccation. However, there was substantial variation in the best predictor variables across the three drought periods.
- We conclude that hydraulic traits and tree height influence growth responses during drought, as recorded in the tree-ring record spanning historical droughts. Thus, these factors can be useful for predicting future drought responses under climate change.

Key words: annual growth; canopy position; drought; Forest Global Earth Observatory (ForestGEO); leaf hydraulic traits; temperate broadleaf deciduous forest; tree height; tree-ring

Introduction

Forests play a critical global role in climate regulation (Bonan, 2008), yet there remains enormous uncertainty as to how the terrestrial carbon sink, which is dominated by forests, will respond to climate change (Friedlingstein et al., 2006). An important aspect of this uncertainty lies with physiological responses of trees to drought (Kennedy et al., 2019). In many forested regions around the world, the risk of severe drought is increasing (Trenberth et al., 2014; Dai et al., 2018), often despite increasing precipitation (Intergovernmental Panel on Climate Change, 2015; Cook et al., 2015). Droughts, intensified by climate change, have been affecting forests worldwide and are expected to continue as one of the most important drivers of forest change in the future (Allen et al., 2010, 2015). Understanding forest responses to drought requires elucidation of how tree size, microenvironment, and species' traits jointly influence individual-level drought resistance, and the extent to which their influence is consistent across droughts. However, it has proven difficult to resolve the many factors affecting tree growth during drought with available forest census data, which only rarely captures extreme drought, and with tree-ring records, which capture multiple droughts but rarely consider the roles of tree size and microenvironment.

Many studies have shown that within species, large trees tend to be more affected by drought. Greater growth reductions for larger trees was first shown on a global scale by Bennett et al. (2015), and subsequent studies have reinforced this finding (*e.g.*, Stovall et al. (2019); Hacket-Pain et al. (2016)). It has yet to be resolved which of several potential underlying mechanisms most strongly shape size trends in drought response. First, tree height may be a primary driver. Taller trees face the biophysical challenge of lifting water greater distances against the effects of gravity and friction (McDowell et al., 2011; McDowell and Allen, 2015; Ryan et al., 2006; Couvreur et al., 2018). Vertical gradients in stem and leaf traits–including smaller and thicker leaves (higher leaf mass per area, LMA), greater resistance to hydraulic dysfunction (*i.e.*, more negative water potential at 50% loss of hydraulic conductivity,more negative P50), and lower hydraulic conductivity at greater heights (Couvreur et al., 2018; Koike et al., 2001; McDowell et al., 2011)–enable trees to become tall (Couvreur et al., 2018). Indeed, tall trees require xylem of greater hydraulic efficiency in their basal portions, such that xylem conduit diameters are wider in taller trees within and across species (Olson et al., 2018; Liu et al., 2019). Wider xylem conduits make large trees more vulnerable to embolism during drought (Olson et al., 2018), and traits conducive to efficient water transport may also lead to poor ability to recover from or re-route water around embolisms (Roskilly et al., 2019). Second, larger trees may have lower drought resistance because they tend to occupy more exposed canopy positions, where they are exposed to higher solar radiation, greater wind speeds, and lower relative humidity (e.g., Koike et al. (2001); Kunert et al. (2017)). Subcanopy trees tend to fare better specifically due to the benefits of a buffered environment (Pretzsch et al., 2018). Third, large trees tend to have larger root systems, which potentially counteracts some of the biophysical challenges they face by allowing greater access to water; however, it appears that this effect is usually insufficient to offset the costs of height and/or crown exposure. Finally, tree size-related responses to drought can be modified by species' traits and their distribution across size classes (Meakem et al., 2018; Liu et al., 2019). Understanding the mechanisms driving the greater relative growth reductions of larger trees during drought will require sorting out the interactive effects of height, canopy position, root water access, and species' traits.

Debates have also arisen regarding the traits influencing tree growth responses to drought. It has been observed that ring-porous species showing higher drought tolerance than diffuse-porous species (Friedrichs et al., 2009; Elliott et al., 2015; Kannenberg et al., 2019), but this classification does not resolve differences

among the many species within each category. Commonly-measured traits including wood density and leaf mass per area (LMA) have been linked to drought responses in some temperate deciduous forests (Abrams, 1990; Guerfel et al., 2009; Hoffmann et al., 2011; Martin-Benito and Pederson, 2015) and other forest biomes around the world (Greenwood et al., 2017). However, in other cases these traits could not explain drought tolerance (Maréchaux et al., 2019), or the direction of response was not always consistent. For instance, higher wood density has been associated with greater drought resistance at a global scale (Greenwood et al., 2017), but it correlated negatively with tree performance during drought in a broadleaf deciduous forest in the southeastern United States (Hoffmann et al., 2011). Thus, the perceived influence of these traits on drought resistance may actually reflect indirect correlations with other traits that more directly drive drought responses (Hoffmann et al., 2011). Recent work has shown a great potential for hydraulic traits to predict growth and mortality responses. Hydraulic traits including water potentials at which percent loss of conductivity surpass a certain threshold ($P50$, $P80$, $P88$) and hydraulic safety margin correlate with drought performance (Anderegg et al., 2018) but are time-consuming to measure and therefore infeasible for predicting or modeling drought responses in highly diverse forests (*e.g.*, in the tropics). More easily measurable leaf hydraulic traits with direct linkage to plant hydraulic function can explain greater variation in plant distribution and function (Medeiros et al., 2019). These include leaf area shrinkage upon desiccation (PLA_{dry}) (Scoffoni et al., 2014) and the leaf water potential at turgor loss point (π_{tlp}), *i.e.,* the water potential at which leaf wilting occurs (Bartlett et al., 2016). The abilities of both PLA_{dry} and π_{tlp} to explain tree performance under drought remains untested.

Here, we examine how tree size, microenvironment characteristics, and species' traits collectively shape drought responses. We test a series of hypotheses and associated specific predictions (Table 1) based on the combination of tree-ring records from three droughts (1966, 1977, 1999), species functional and hydraulic trait measurements, and census data from a large forest dynamics plot in Virginia, USA. First, we focus on the role of tree size and its interaction with microenvironment. We test whether, consistent with most forests globally, larger-diameter trees tend to have lower drought resistance (Rt) in this forest, which is in a region (eastern North America) represented by only two studies in the global review of Bennett et al. (2015). We then test hypotheses designed to disentangle the relative importance of tree height; crown exposure; and soil water availability, which should be greater for larger trees in dry but not in perpetually wet microsites. Second, we focus on the role of species' functional and hydraulic traits, testing the hypothesis that species' traits—particularly leaf hydraulic traits—predict Rt. We test predictions that drought resistance is higher in ring-porous than semi-ring and diffuse-porous species, that it is correlated with wood density–either postively (Greenwood et al., 2017) or negatively (Hoffmann et al., 2011)– and positively correlated with LMA, and that hydraulic leaf traits including PLA_{dry} and π_{tlp} are better predictors.

Materials and Methods

Study site

Research was conducted at the 25.6-ha ForestGEO (Forest Global Earth Observatory) study plot at the Smithsonian Conservation Biology Institute (SCBI) in Virginia, USA (38°53'36.6"N, 78°08'43.4"W) (Bourg et al., 2013; Anderson-Teixeira et al., 2015a). SCBI is located in the central Appalachian Mountains near the northern boundary of Shenandoah National Park. Elevations range from 273 to 338 m above sea level with a topographic relief of 65m (Bourg et al., 2013). Climate is humid temperate, with mean annual temperature of 12.7°C and precipitation of 1005 mm during our study period (1960-2009; source: CRU TS v.4.01; Harris

et al. (2014)). Dominant tree taxa within this secondary forest include *Liriodendron tulipifera*, oaks (*Quercus* spp.), and hickories (*Carya* spp.).

Data collection and preparation

Within or just outside the ForestGEO plot, we collected data on a suite of variables including tree size, microenvironment characteristics, and species traits (Table 2). The SCBI ForestGEO plot was censused in 2008, 2013, and 2018 following standard ForestGEO protocols, whereby all free-standing woody stems $\geq$ 1cm diameter at breast height (DBH) were mapped, tagged, measured at DBH, and identified to species (Condit, 1998). From this census data, we used measurements of DBH from 2008 to calculate historical DBH and data for all stems $\geq$ 10cm to analyze functional trait composition relative to tree height (all analyses described below). Census data are available through the ForestGEO data portal (www.forestgeo.si.edu).

We analyzed tree-ring data (cambial growth increment) from 571 trees representing the twelve species with the greatest contributions to woody aboveground net primary productivity ($ANPP_{stem}$), which together comprised 97% of study plot $ANPP_{stem}$ between 2008 and 2013 (Helcoski et al., 2019) (Fig. **S1**). Cores were collected within the ForestGEO plot at breast height (1.3m) in 2010-2011 or 2016-2017. In 2010-2011, cores were collected from randomly selected live trees of each species that had at least 30 individuals $\geq$ 10 cm DBH (Bourg et al., 2013). In 2016-2017, cores were collected from all trees found dead during annual mortality censuses (Gonzalez-Akre et al., 2016). Cores were sanded, measured, and crossdated using standard procedures, as detailed in (Helcoski et al., 2019). The resulting chronologies were published in Zenodo (DOI: 10.5281/zenodo.2649302) in association with Helcoski et al. (2019).

For each cored tree, we combined tree-ring records and allometric equations of bark thickness to retroactively calculate DBH for the years 1950-2009. Prior DBH was estimated using the following equation:

$$DBH_Y = DBH_{2008} - 2 * \left[\sum_{year=Y}^{2008} (r_{ring,Y}) - r_{bark,Y} + r_{bark,2008} \right]$$

Here, Y denotes the year of interest, r_{ring} denotes ring width derived from cores, and r_{bark} denotes bark thickness. Bark thickness was estimated from species-specific allometries based on the bark thickness data from the site (Anderson-Teixeira et al., 2015b). Specifically, we used linear regression on log-transformed data to relate bark thickness to diameter inside bark from 2008 data (Table S1), which were then used to determine bark thickness in the retroactive calculation of DBH.

Tree heights (H) were measured by several researchers for a variety of purposes between 2012 to 2019 (n=1,518 trees). Measurement methods included direct measurements using a collapsible measurement rod on small trees (NEON, 2018) or a tape measure on recently fallen trees (this study); geometric calculations using clinometer and tape measure (Stovall et al., 2018a) or digital rangefinders (Anderson-Teixeira et al., 2015b; NEON, 2018); and ground-based LiDAR (Stovall et al., 2018b). Rangefinders used either the tangent method (Impulse 200LR, TruPulse 360R) or the sine method (Nikon ForestryPro) for calculating heights. Both methods are associated with some error (Larjavaara and Muller-Landau, 2013), but in this instance there was no clear advantage of one or the other. Measurements from the National Ecological Observatory Network (NEON) were collected near the ForestGEO plot following standard NEON protocol, whereby vegetation of short stature was measured with a collapsible measurement rod, and taller trees with a rangefinder (NEON, 2018). Species-specific height allometries were developed (Table S2) using logarithmic regression

($ln[H]$ $ln[DBH]$). For species with insufficient height data to create reliable species-specific allometries, heights were calculated from an equation developed by combining the height measurements across all species.

Crown position–a categorical variable including dominant, co-dominant, intermediate, and suppressed–was recorded for all cored trees that remained standing during the growing season of 2018 following the protocol of Jennings et al. (1999). While some tree crowns undoubtedly changed position over the past several decades, in this case the bias would be unlikely to result in false acceptance of our hypothesis (*i.e.*, type I error unlikely, type II error possible), making our hypothesis test conservative. An analysis of crown position relative to height (Fig. **2d**) and height changes since the beginning of the study period indicated that changes between focal drought years (1966, 1977, and 1999; see below) were fairly small relative to differences among canopy positions (Fig. **S3**), with average tree height growth confined to ~0.82 m from 1966 to 1977, ~1.45 m from 1977 to 1999, and ~1.97 m from 1999 to 2018. However, dominant and co-dominant trees were similar in height (Figs. **2d**, **S3**).

Topographic wetness index (TWI) was calculated using the dynatopmodel package in R (Fig. **S1**) (Metcalfe et al., 2018). Originally developed by Beven and Kirkby (1979), TWI was part of a hydrological run-off model and has since been used for a number of purposes in hydrology and ecology (Sørensen et al., 2006). TWI calculation depends on an input of a digital elevation model (DEM; ~3.7 m resolution from the elevatr package (Hollister, 2018)), and from this yields a quantitative assessment defined by how "wet" an area is, based on areas where run-off is more likely. From our observations in the plot, TWI performed better at categorizing wet areas than the Euclidean distance from the stream.

Hydraulic traits were collected in August 2018 (Table 3). We sampled small sun-exposed branches up to eight meters above ground from three individuals of each species in and around the ForestGEO plot. Sampled branches were re-cut under water at least two nodes above the original cut and re-hydrated overnight in covered buckets under opaque plastic bags before measurements were taken. Rehydrated leaves taken towards the apical end of the branch (n=3 per individual: small, medium, and large) were scanned, weighed, dried at 60° C for $\geq$ 48 hours, and then re-scanned and weighed. Leaf area was calculated from scanned images using the LeafArea R package (Katabuchi, 2019). LMA was calculated as the ratio of leaf dry mass to fresh area. PLA_{dry} was calculated as the percent loss of area between fresh and dry leaves. wood density was calculated for ~1cm diameter stem samples (bark and pith removed) as the ratio of dry weight to volume, which was estimated using Archimedes' displacement. We used the rapid determination method of Bartlett et al. (2012) to estimate osmotic potential at turgor loss point (π_{tlp}). Briefly, two 4 mm diameter leaf discs were cut from each leaf, tightly wrapped in foil, submerged in liquid nitrogen, perforated 10-15 times with a dissection needle, and then measured using a vapour pressure osmometer (VAPRO 5520, Wescor, Logan, UT, USA). Osmotic potential (π_{osm}) given by the osmometer was used to estimate (π_{tlp}) using the equation $\pi_{tlp} = 0.832\pi_{osm}^{-0.631}$ (Bartlett et al., 2012).

To characterize how environmental conditions vary with height, data were obtained from the NEON tower located <1km from the study area. We used wind speed, relative humidity, and air temperature data, all measured over a vertical profile spanning heights from 7.2 m to above the top of the tree canopy (31.0 or 51.8m, depending on censor), for the years 2016-2018 (NEON, 2018). After filtering for missing and outlier values, we determined the daily minima and maxima, which we then aggregated at the monthly scale.

Identifying drought years

We identified droughts within the time period 1950-2009, defining drought (Slette et al., 2019) as events with

both anomalously dry peak growing season climatic conditions and widespread reductions in tree growth, *i.e.*, droughts that substantially impacted the forest community. We identified three drought years: 1966, 1977, and 1999 (Figs. **1**, **S2**, Table S3). These were the three years with the lowest Palmer Drought Severity Index (PDSI) during May-August (MJJA; Table S3), which were identified by Helcoski et al. (2019) as the months of the current year to which annual tree growth was most sensitive at this site. PDSI divisional data for Northern Virginia were obtained from NOAA (https://www7.ncdc.noaa.gov/CDO/CDODivisionalSelect.jsp) in December 2017. These were also years with widespread tree growth reduction ("pointer years"), here defined as those where >25% of the cored trees experienced >30% reduction in basal area increment (BAI) relative to the previous 5 years, following the drought resistance (Rt) metric of (Lloret et al., 2011). Pointer years were identified using the pointRes package in R (van der Maaten-Theunissen and van der Maaten, 2016). In addition to the focal drought years, 1991 also met this critera (26.5% of trees experienced >30% growth reduction, mean resistance= -13.8%) but was excluded because it was not among the driest of the time period (Table S3). Rather, the severity of growth reduction could probably be explained in large part by defoliation by gypsy moths (*Lymantria dispar* L.), which was documented to have strongly impacted *Quercus* spp. in the area from approximately 1988 through 1995 (Twery, 1991).

The droughts differed in intensity and antecedent moisture conditions (Fig. **S2**, Table S3). The 1966 drought was preceded by two years of moderate drought during the growing season and severe to extreme drought starting the previous fall and in August reached the lowest growing season $PDSI$ (-4.82) of the three droughts. The 1977 drought was the least intense throughout the growing season, and it was preceded by 2.5 years of near-normal conditions, making it the mildest of the three droughts. The 1999 drought was preceded by wetter than average conditions until the previous June, but reached the lowest PDSI during May-July (-4.53).

Statistical Analysis

For each drought year, we calculated drought resistance (Rt) as the ratio of BAI during drought to the mean BAI over the five years preceding the drought (Lloret et al., 2011). Thus, Rt values <1 and >1 indicate growth reductions and increases, respectively. Analyses focused on testing the predictions presented in Table 1, with Rt as the response variable. The general statistical model for hypothesis testing was a mixed effects model with Rt as the response variable, tree nested within species as a random effect, and one or more independent variables as fixed effects. Mixed effects models were implemented in the lme4 package in R (Bates et al., 2019). We used AICc to assess model selection, and conditional/marginal R-squared to assess model fit, implmented in the AICcmodavg package in R (Mazerolle and portions of code contributed by Dan Linden., 2019).

Models were run for all drought years combined and for each drought year individually. In order to determine the relative importance of each predictor variable individually, we first implemented models with the variable in question as a fixed effect, along with drought year (for model with all drought years combined) and $ln[H]$ (included in null models because of it's substantial influence). Variables were considered to have significant influence on Rt when AICc was reduced by ≥ 2 units relative to the corresponding null model lacking that variable (Table 4).

We then determined the best full models for predicting Rt for each individual drought year and for all years combined. Candidate variables were selected, based on the single-variable tests, as those whose addition to a corresponding null model improved fit (at dAICc ≥ 1.0) in at least one drought year (Table 4). We compared

models with all possible combinations of candidate variables and identified the full set of models within dAICc=1 of the very top model (that with lowest AICc), henceforth referred to as "full models". When a variable appeared in all top models and the sign of the coefficient was consistent across models, we viewed this as support for the acceptance/rejection of the associated prediction by the full models. If the variable appeared in only some of the models, we considered this partial support/rejection.

All analysis beyond basic data collection was performed using R version 3.5.3 (R Core Team, 2019). All data, code, and results are available through the SCBI-ForestGEO organization on GitHub (https://github.com/SCBI-ForestGEO: SCBI-ForestGEO-Data and McGregor_climate-sensitivity-variation repositories), with static versions corresponding to data and analyses presented here archived in Zenodo (DOIs: 10.5281/zenodo.3604993 and [TBD], respectively.

Results

Community-level drought responses

At the community level, cored trees showed substantial growth reductions in all three droughts, with a mean Rt of 0.86 in 1966 and 1999, and 0.84 in 1977 (Fig. **1b**). In each drought, roughly 30% of the cored trees had growth reductions of >30% ($Rt \leq 0.7$): 29% in 1966, 32% in 1977, and 27% in 1999. However, some individuals exhibited increased growth, *i.e.*, $Rt > 1.0$: 26% of trees in 1966, 22% in 1977, and 26% in 1999.

Tree size, microenvironment, and drought resistance

Larger-diameter trees showed stronger growth reductions during drought when evaluating the three drought years together and for 1966 individually, although DBH was not significant during 1977 or 1999 individually (Tables 1, 4). The same held true for $ln[H]$ in single-variable tests (Tables 1, 4). When combined with other predictor variables in the full models, $ln[H]$ appeared, with negative coefficient, in all full models for the three droughts combined, in the 1966 model, and in one of the two models for 1999 (Tables 1, 5).

Crown position varied as expected with height (dominant > co-dominant > intermediate > suppressed), but with substantial variation (Fig. **2d**). When considered alone, crown position had a significant response only in the 1966 drought, during which trees with dominant crown position had the lowest Rt. Crown position was a much poorer predictor of Rt than was height in the single-variable tests (Table 4), lending little overall support to the hypothesis that crown exposure reduces Rt (Table 1). When height was included in the model, crown position was a significant predictor in the 1999 drought, with lowest Rt for suppressed and then intermediate trees. Crown position was included in some of the full models (Table 5). In 1977, where height was not included in the full model, dominant trees had the lowest Rt, and suppressed trees the highest. In contrast, in full models including both height and crown position (all droughts and 1999), the lowest Rt was in suppressed, followed by intermediate, trees.

In the years for which we have vertical profiles in climate data (2016-2018), taller trees–or those in dominant crown positions– were generally exposed to higher evaporative demand during the peak growing season months (May-August; Fig. **2**). Specifically, maximum daily wind speeds were significantly higher above the top of the canopy (40-50m) than within and below (10-30m) (Fig. **2a**). Relative humidity was also somewhat lower during June-August, ranging from ~50-80% above the canopy and ~60-90% in the understory (Fig. **2b**). Air temperature did not vary across the vertical profile (Fig. **2c**).

Rt was negatively correlated with $ln[TWI]$ (Tables 4-5), rejecting the idea that trees in moist microsites

would be less affected by drought. Nevertheless, we tested for a negative $ln[H] * ln[TWI]$ interaction, which could indicate that smaller trees (with smaller rooting volume) are more susceptible to drought in drier microenvironments with a deeper water table. This hypothesis was rejected as the $ln[H] * ln[TWI]$ interaction was never significant (Table 4).

Species' traits and drought resistance

The leaf hydraulic traits PLA_{dry} and π_{tlp} were linked to drought responses, whereas the other traits considered had insignficant and/or inconsistent correlations to Rt (Tables 1,4,5). In the single-variable tests, LMA and wood density were never significantly associated with Rt (Table 4) and were excluded from the full models. In contrast, xylem porosity, PLA_{dry}, and π_{tlp} all explained modest amounts of variation (dAIC > 1.0) during at least one of the three droughts (Table 4). Xylem porosity was not significant for all droughts combined and had contrasting effects in the individual droughts: whereas ring-porous species had higher Rt than diffuse- and semi-ring- porous species in the 1966 and 1999 droughts, they had lower Rt in 1977 (Tables 4,5). PLA_{dry} was a strong predictor for 1966 and all droughts combined, with consistently negative coefficients (Table 4). Similarly, PLA_{dry} was consistently included, with negative coefficient, in full models for the three droughts combined and for the 1966 and 1977 droughts individually (Table 5). π_{tlp} was not significant in any single-variable tests; however, coefficients were consistently negative (Table 4) and π_{tlp} was included in the top full model for all droughts combined and for the 1977 and 1999 droughts individually (Table 5).

Discussion

Tree size, microenvironment, and hydraulic traits shaped tree growth responses across three droughts at our study site (Table 1). The greater susceptibility of larger trees to drought, similar to forests worldwide (Bennett et al., 2015), was driven primarily by their height rather than crown exposure (Liu and Muller, 1993; Stovall et al., 2019). We found only a marginal additional effect of crown exposure, with a tendency for lowest Rt among the most exposed (dominant) and suppressed trees. The negative effect of height on Rt held after accounting for species' traits. There was no evidence that soil water availability increased drought resistance; in contrast, trees in wetter topographic positions had lower Rt (Zuleta et al., 2017; Stovall et al., 2019), and the larger potential rooting volume of large trees provided no advantage in the drier microenvironments. Drought resistance was not consistently linked to species' LMA, wood density, or xylem type (ring- vs. diffuse porous), but was negatively correlated with leaf hydraulic traits (PLA_{dry}, π_{tlp}) in the top overall model and the top models for two of the three individual droughts. This is the first report to our knowledge linking PLA_{dry} and π_{tlp} to growth reduction during drought. The direction of responses was mostly consistent across droughts, supporting the premise that they were driven by fundamental physiological mechanisms. However, the strengths of each predictor varied across droughts (Tables 4-5), indicating that drought characteristics interact with tree size, microenvironment, and traits to shape which individuals are most affected. These findings advance our knowledge of the factors that make trees vulnerable to growth declines during drought–and, by extension, likely make them more vulnerable to mortality (Sapes et al., 2019).

The droughts considered here were of a magnitude that has occurred with an average frequency of approximately once every 10-15 years (Fig. **1a**, Helcoski et al. (2019)) and had substantial but not devastating impacts on tree growth (Fig. **1b**). These droughts were classified as severe (1977) or extreme (1966, 1999) according to the PDSI metric and have been linked to tree mortality in the eastern United States

(Druckenbrod et al., 2019); however, extreme, multiannual droughts or so-called "megadroughts" of the type that have triggered massive tree die-off in other regions (e.g., Allen et al. (2010); Stovall et al. (2019)) have not occurred in the Eastern United States within the past several decades (Clark et al., 2016). Of the droughts considered here, the 1966 drought, which was preceded by two years of dry conditions (Fig. **S2**), severely stressed a larger portion of trees (Fig. **1b**). The tendency for large trees to have lowest resistance was most pronounced in this drought, consistent with other findings that this physiological response increases with drought severity (Bennett et al., 2015; Stovall et al., 2019). Across all three droughts, the majority of trees experienced reduced growth, but a substantial portion had increased growth (Fig. **1b**), potentially due to decreased leaf area of competitors during the drought. It is likely because of the moderate impact of these droughts, along with other factors influencing tree growth, that our best models characterize only a modest amount of variation: 11-13% for all droughts combined, and 21-26% for each individual drought (Table 5).

Our analysis indicates that tree height has a stronger influence on drought response than does canopy position (Tables 1,4,5). This is consistent with, and reinforces, previous findings that biophysical constraints make it impossible for trees to efficiently transport water to great heights and simultaneously maintain strong resistance and resilience to drought-induced embolism (Olson et al., 2018; Couvreur et al., 2018; Roskilly et al., 2019). However, the collinearity between the two variables (Fig. **2d**) makes it impossible to confidently partition causality. Taller trees are more likely to be in dominant canopy positions (Fig. **2d**) and, largely as a consequence of their position relative to others, face different microenvironments (Fig. **2a-b**). Even under non-drought conditions, evaporative demand and maximum leaf temperatures increase with tree height (Smith and Nobel, 1977; Bretfeld et al., 2018; Kunert et al., 2017), and such conditions would incur additional stress during drought, when solar radiation tends to be higher and less water is available for evaporative cooling of the leaves. However, some decoupling between height and canopy position is introduced by the configuration of neighboring trees (Fig. **2d**) (Muller-Landau et al., 2006), and height was an overall stronger predictor of drought response than crown position (Tables 1,4,5). Belowground, taller trees would tend to have larger root systems, but the potentially greater access to water did not override the vulnerability conferred by height–and, in fact, greater moisture access in non-droought years (here, higher TWI) appears to make trees more vulnerable to drought (Zuleta et al., 2017; Stovall et al., 2019).

Our analysis has the limitation that canopy positions were recorded in 2018, as opposed to the years of the droughts. However, because trees would generally advance towards more dominant positions as they grow and as neighbors die, changing canopy positions would bias against the acceptance of our hypothesis. The implication is that dominant crown positions did have a marginally negative influence on *Rt*, which makes sense in light of the vertical environmental gradients described above and agrees with previous studies showing lower drought resistance in more exposed trees (Suarez et al., 2004; Scharnweber et al., 2019). It is safe to assume that currently suppressed trees were suppressed throughout our analysis period, and their relatively low *Rt* (after accounting for height effects) is real, perhaps as a result of competition (Sohn et al., 2016). The observed height-sensitivity of *Rt*, together with the lack of advantage to large stature in drier topographic positions, agrees with the concept that physiological limitations to transpiration under drought shift from soil water availability to the plant-atmosphere interface as forests age (Bretfeld et al., 2018), such that tall, dominant trees are the most sensitive in mature forests. Additional research comparing drought responses of young and old forest stands, along with short and tall isolated trees, would be valuable for more clearly disentangling the roles of tree height and crown exposure.

The development of tree-ring chronologies for the twelve most dominant tree species at our site (Helcoski

et al., 2019; Bourg et al., 2013) gave us the sample size to compare historical drought responses across species and associated traits at a single site (see also Elliott et al., 2015). Concerted measurement of leaf hydraulic traits of emerging importance (Scoffoni et al., 2014; Bartlett et al., 2016; Medeiros et al., 2019) allowed novel insights into the role of hydraulic traits in shaping drought response. The finding that PLA_{dry} and π_{tlp} can be useful for predicting drought responses of tree growth (Tables 1,4,5) is both novel and consistent with previous studies linking these traits to habitat and drought tolerance. Previous studies have demonstrated that π_{tlp} and PLA_{dry} are physiologically meaningful traits linked to species distribution along moisture gradients (Maréchaux et al., 2015; Fletcher et al., 2018; Medeiros et al., 2019; Simeone et al., 2019; Rosas et al., 2019), and our findings indicate that these traits also influence drought responses. Furthermore, the observed linkage of π_{tlp} to Rt in this forest aligns with observations in the Amazon that π_{tlp} is higher in drought-intolerant than drought-tolerant plant functional types and adds support to the idea that this trait is useful for categorizing and representing species' drought responses in models (Powell et al., 2017). Because both PLA_{dry} and π_{tlp} can be measured relatively easily (Bartlett et al., 2012; Scoffoni et al., 2014), they hold promise for predicting drought growth responses across diverse forests. The importance of predicting drought responses from species traits increases with tree species diversity; whereas it is feasible to study drought responses for all dominant species in most boreal and temperate forests (e.g., this study), this becomes difficult to impossible for species that do not form annual rings, and for diverse tropical forests. Although progress is being made for the tropics (Schöngart et al., 2017), a full linkage of hydraulic traits to drought responses would be invaluable for forecasting how little-known species and whole forests will respond to future droughts (Powell et al., 2017).

As climate change drives increasing drought in many of the world's forests (Trenberth et al., 2014; Intergovernmental Panel on Climate Change, 2015), the fate of forests and their climate feedbacks will be shaped by the biophysical and physiological drivers observed here. Large trees have been disproportionately impacted by strong drought in forests around the world (Bennett et al., 2015; Stovall et al., 2019), and we show, at least at this site, that this is primarily driven by their height with some contributions from canopy position. The distinction is important because it suggests that height *per se* makes trees vulnerable, even if their crowns are somewhat protected by neighbors, whereas shorter solitary trees or the dominant trees in young forests that recently established after logging or natural disturbances should be less vulnerable. This would suggest that, all else being equal, mature forests would be more vulnerable to drought than young forests with short trees; however, root water access may limit the young forests (Bretfeld et al., 2018), and species traits often shift as forests age. Early- to mid- successional species at our site (*Liriodendron tulipifera*, *Quercus spp.*, *Fraxinus americana*) display a mix of traits conferring drought tolerance and resistance (Table 3), and further research on how hydraulic traits and drought vulnerability change over the course of succession would be valuable for addressing how drought tolerance changes as forests age (e.g. Rodríguez-Catón et al., 2015). In the meantime, the results of this study advance our knowledge of the factors conferring drought vulnerability and resistance in a mature forest, opening the door for more accurate forecasting of forest responses to future drought.

Acknowledgements

We especially thank the numerous researchers who helped to collect the data used here, in particular Jennifer C. McGarvey, Jonathan R. Thompson, and Victoria Meakem for original collection and processing of cores. Thanks also to Camila D. Medeiros for guidance on hydraulic and functional trait measurements, Edward

Brzostek's lab for collaboration on leaf sampling, and Maya Prestipino for data collection. Funding for the establishment of the SCBI ForestGEO Large Forest Dynamics Plot was provided by the Smithsonian-led Forest Global Earth Observatory (ForestGEO), the Smithsonian Institution, and the HSBC Climate Partnership. This study was funded by ForestGEO, a Virginia Native Plant Society grant to KAT and AJT, and support from the Harvard Forest and National Science Foundation which supports the PalEON project (NSF EF-1241930) for NP.

Author Contribution

KAT, IM, and AJT designed the research. Tree-ring chronologies were developed by RH under guidance of AJT and NP. Trait data was collected by IM, JZ under guidance of NK and LS. Other plot data were collected by IM, AS, EGA, and NB under guidance of EGA and WM. Data analyses were performed by IM under guidance of KAT and VH. KAT and IM interpreted the results. IM and KAT wrote the first draft of manuscript, and all authors contributed to revisions.

Supplementary Information

Table S1: Species-specific bark thickness regression equations

Table S2: Species-specific height regression equations

Table S3: Palmer drought severity index (PDSI) by month for focal droughts

Figure S1: Map of ForestGEO plot showing TWI and location of cored trees

Figure S2: Time series of Palmer Drought Severity Index (PDSI) for the 2.5 years prior to each focal drought

Figure S3: Height by canopy position across the three focal droughts and in the year of measurement (2018)

References

Abrams, M. D. (1990). Adaptations and responses to drought in Quercus species of North America. *Tree Physiology*, 7(1-2-3-4):227–238.

Allen, C. D., Breshears, D. D., and McDowell, N. G. (2015). On underestimation of global vulnerability to tree mortality and forest die-off from hotter drought in the Anthropocene. *Ecosphere*, 6(8):art129.

Allen, C. D., Macalady, A. K., Chenchouni, H., Bachelet, D., McDowell, N., Vennetier, M., Kitzberger, T., Rigling, A., Breshears, D. D., Hogg, E. H. T., Gonzalez, P., Fensham, R., Zhang, Z., Castro, J., Demidova, N., Lim, J.-H., Allard, G., Running, S. W., Semerci, A., and Cobb, N. (2010). A global overview of drought and heat-induced tree mortality reveals emerging climate change risks for forests. *Forest Ecology and Management*, 259(4):660–684.

Anderegg, W. R. L., Konings, A. G., Trugman, A. T., Yu, K., Bowling, D. R., Gabbitas, R., Karp, D. S., Pacala, S., Sperry, J. S., Sulman, B. N., and Zenes, N. (2018). Hydraulic diversity of forests regulates ecosystem resilience during drought. *Nature*, 561(7724):538–541.

Anderson-Teixeira, K. J., Davies, S. J., Bennett, A. C., Gonzalez-Akre, E. B., Muller-Landau, H. C., Wright, S. J., Salim, K. A., Zambrano, A. M. A., Alonso, A., Baltzer, J. L., Basset, Y., Bourg, N. A., Broadbent, E. N., Brockelman, W. Y., Bunyavejchewin, S., Burslem, D. F. R. P., Butt, N., Cao, M., Cardenas, D.,

Chuyong, G. B., Clay, K., Cordell, S., Dattaraja, H. S., Deng, X., Detto, M., Du, X., Duque, A., Erikson, D. L., Ewango, C. E. N., Fischer, G. A., Fletcher, C., Foster, R. B., Giardina, C. P., Gilbert, G. S., Gunatilleke, N., Gunatilleke, S., Hao, Z., Hargrove, W. W., Hart, T. B., Hau, B. C. H., He, F., Hoffman, F. M., Howe, R. W., Hubbell, S. P., Inman-Narahari, F. M., Jansen, P. A., Jiang, M., Johnson, D. J., Kanzaki, M., Kassim, A. R., Kenfack, D., Kibet, S., Kinnaird, M. F., Korte, L., Kral, K., Kumar, J., Larson, A. J., Li, Y., Li, X., Liu, S., Lum, S. K. Y., Lutz, J. A., Ma, K., Maddalena, D. M., Makana, J.-R., Malhi, Y., Marthews, T., Serudin, R. M., McMahon, S. M., McShea, W. J., Memiaghe, H. R., Mi, X., Mizuno, T., Morecroft, M., Myers, J. A., Novotny, V., Oliveira, A. A. d., Ong, P. S., Orwig, D. A., Ostertag, R., Ouden, J. d., Parker, G. G., Phillips, R. P., Sack, L., Sainge, M. N., Sang, W., Sri-ngernyuang, K., Sukumar, R., Sun, I.-F., Sungpalee, W., Suresh, H. S., Tan, S., Thomas, S. C., Thomas, D. W., Thompson, J., Turner, B. L., Uriarte, M., Valencia, R., Vallejo, M. I., Vicentini, A., Vrška, T., Wang, X., Wang, X., Weiblen, G., Wolf, A., Xu, H., Yap, S., and Zimmerman, J. (2015a). CTFS-ForestGEO: a worldwide network monitoring forests in an era of global change. *Global Change Biology*, 21(2):528–549.

Anderson-Teixeira, K. J., McGarvey, J. C., Muller-Landau, H. C., Park, J. Y., Gonzalez-Akre, E. B., Herrmann, V., Bennett, A. C., So, C. V., Bourg, N. A., Thompson, J. R., McMahon, S. M., and McShea, W. J. (2015b). Size-related scaling of tree form and function in a mixed-age forest. *Functional Ecology*, 29(12):1587–1602.

Bartlett, M. K., Klein, T., Jansen, S., Choat, B., and Sack, L. (2016). The correlations and sequence of plant stomatal, hydraulic, and wilting responses to drought. *Proceedings of the National Academy of Sciences*, 113(46):13098–13103.

Bartlett, M. K., Scoffoni, C., Ardy, R., Zhang, Y., Sun, S., Cao, K., and Sack, L. (2012). Rapid determination of comparative drought tolerance traits: using an osmometer to predict turgor loss point. *Methods in Ecology and Evolution*, 3(5):880–888.

Bates, D., Maechler, M., Bolker, B., and Walker, S. (2019). *lme4: Linear Mixed-Effects Models using 'Eigen' and S4*. R package version 1.1-21.

Bennett, A. C., McDowell, N. G., Allen, C. D., and Anderson-Teixeira, K. J. (2015). Larger trees suffer most during drought in forests worldwide. *Nature Plants*, 1(10):15139.

Beven, K. J. and Kirkby, M. J. (1979). A physically based, variable contributing area model of basin hydrology / Un modèle à base physique de zone d'appel variable de l'hydrologie du bassin versant. *Hydrological Sciences Bulletin*, 24(1):43–69.

Bonan, G. B. (2008). Forests and Climate Change: Forcings, Feedbacks, and the Climate Benefits of Forests. *Science*, 320(5882):1444–1449.

Bourg, N. A., McShea, W. J., Thompson, J. R., McGarvey, J. C., and Shen, X. (2013). Initial census, woody seedling, seed rain, and stand structure data for the SCBI SIGEO Large Forest Dynamics Plot. *Ecology*, 94(9):2111–2112.

Bretfeld, M., Ewers, B. E., and Hall, J. S. (2018). Plant water use responses along secondary forest succession during the 2015–2016 El Niño drought in Panama. *New Phytologist*, 219(3):885–899.

Clark, J. S., Iverson, L., Woodall, C. W., Allen, C. D., Bell, D. M., Bragg, D. C., D'Amato, A. W., Davis, F. W., Hersh, M. H., Ibanez, I., Jackson, S. T., Matthews, S., Pederson, N., Peters, M., Schwartz, M. W., Waring, K. M., and Zimmermann, N. E. (2016). The impacts of increasing drought on forest dynamics, structure, and biodiversity in the United States. *Global Change Biology*, 22(7):2329–2352.

Condit, R. (1998). *Tropical Forest Census Plots: Methods and Results from Barro Colorado Island, Panama and a Comparison with Other Plots*. Springer Berlin Heidelberg, Berlin, Heidelberg.

Cook, B. I., Ault, T. R., and Smerdon, J. E. (2015). Unprecedented 21st century drought risk in the American Southwest and Central Plains. *Science Advances*, 1(1):e1400082.

Couvreur, V., Ledder, G., Manzoni, S., Way, D. A., Muller, E. B., and Russo, S. E. (2018). Water transport through tall trees: A vertically explicit, analytical model of xylem hydraulic conductance in stems. *Plant, Cell & Environment*, 41(8):1821–1839.

Dai, A., Zhao, T., and Chen, J. (2018). Climate Change and Drought: a Precipitation and Evaporation Perspective. *Current Climate Change Reports*, 4(3):301–312.

Druckenbrod, D. L., Martin-Benito, D., Orwig, D. A., Pederson, N., Poulter, B., Renwick, K. M., and Shugart, H. H. (2019). Redefining temperate forest responses to climate and disturbance in the eastern United States: New insights at the mesoscale. *Global Ecology and Biogeography*, 28(5):557–575.

Elliott, K. J., Miniat, C. F., Pederson, N., and Laseter, S. H. (2015). Forest tree growth response to hydroclimate variability in the southern Appalachians. *Global Change Biology*, 21(12):4627–4641.

Fletcher, L. R., Cui, H., Callahan, H., Scoffoni, C., John, G. P., Bartlett, M. K., Burge, D. O., and Sack, L. (2018). Evolution of leaf structure and drought tolerance in species of Californian Ceanothus. *American Journal of Botany*, 105(10):1672–1687.

Friedlingstein, P., Cox, P., Betts, R., Bopp, L., von Bloh, W., Brovkin, V., Cadule, P., Doney, S., Eby, M., Fung, I., Bala, G., John, J., Jones, C., Joos, F., Kato, T., Kawamiya, M., Knorr, W., Lindsay, K., Matthews, H. D., Raddatz, T., Rayner, P., Reick, C., Roeckner, E., Schnitzler, K.-G., Schnur, R., Strassmann, K., Weaver, A. J., Yoshikawa, C., and Zeng, N. (2006). Climate–Carbon Cycle Feedback Analysis: Results from the C4MIP Model Intercomparison. *Journal of Climate*, 19(14):3337–3353.

Friedrichs, D. A., Trouet, V., Büntgen, U., Frank, D. C., Esper, J., Neuwirth, B., and Löffler, J. (2009). Species-specific climate sensitivity of tree growth in Central-West Germany. *Trees*, 23(4):729.

Gonzalez-Akre, E., Meakem, V., Eng, C.-Y., Tepley, A. J., Bourg, N. A., McShea, W., Davies, S. J., and Anderson-Teixeira, K. (2016). Patterns of tree mortality in a temperate deciduous forest derived from a large forest dynamics plot. *Ecosphere*, 7(12):e01595.

Greenwood, S., Ruiz-Benito, P., Martínez-Vilalta, J., Lloret, F., Kitzberger, T., Allen, C. D., Fensham, R., Laughlin, D. C., Kattge, J., Bönisch, G., Kraft, N. J. B., and Jump, A. S. (2017). Tree mortality across biomes is promoted by drought intensity, lower wood density and higher specific leaf area. *Ecology Letters*, 20(4):539–553.

Guerfel, M., Baccouri, O., Boujnah, D., Chaïbi, W., and Zarrouk, M. (2009). Impacts of water stress on gas exchange, water relations, chlorophyll content and leaf structure in the two main Tunisian olive (Olea europaea L.) cultivars. *Scientia Horticulturae*, 119(3):257–263.

Hacket-Pain, A. J., Cavin, L., Friend, A. D., and Jump, A. S. (2016). Consistent limitation of growth by high temperature and low precipitation from range core to southern edge of European beech indicates widespread vulnerability to changing climate. *European Journal of Forest Research*, 135(5):897–909.

Harris, I., Jones, P. D., Osborn, T. J., and Lister, D. H. (2014). Updated high-resolution grids of monthly climatic observations – the CRU TS3.10 Dataset. *International Journal of Climatology*, 34(3):623–642.

Helcoski, R., Tepley, A. J., Pederson, N., McGarvey, J. C., Meakem, V., Herrmann, V., Thompson, J. R., and Anderson-Teixeira, K. J. (2019). Growing season moisture drives interannual variation in woody productivity of a temperate deciduous forest. *New Phytologist*, 0(0).

Hoffmann, W. A., Marchin, R. M., Abit, P., and Lau, O. L. (2011). Hydraulic failure and tree dieback are associated with high wood density in a temperate forest under extreme drought. *Global Change Biology*, 17(8):2731–2742.

Hollister, J. (2018). *elevatr: Access Elevation Data from Various APIs*. R package version 0.2.0.

Intergovernmental Panel on Climate Change (2015). *Climate Change 2014: Impacts, Adaptation and Vulnerability: Working Group II Contribution to the IPCC Fifth Assessment Report. Volume 2 Volume 2*. OCLC: 900892773.

Jennings, S. B., Brown, N. D., and Sheil, D. (1999). Assessing forest canopies and understorey illumination: canopy closure, canopy cover and other measures. *Forestry: An International Journal of Forest Research*, 72(1):59–74.

Kannenberg, S. A., Novick, K. A., Alexander, M. R., Maxwell, J. T., Moore, D. J. P., Phillips, R. P., and Anderegg, W. R. L. (2019). Linking drought legacy effects across scales: From leaves to tree rings to ecosystems. *Global Change Biology*, 0(ja).

Katabuchi, M. (2019). *LeafArea: Rapid Digital Image Analysis of Leaf Area*. R package version 0.1.8.

Kennedy, D., Swenson, S., Oleson, K. W., Lawrence, D. M., Fisher, R., Costa, A. C. L. d., and Gentine, P. (2019). Implementing Plant Hydraulics in the Community Land Model, Version 5. *Journal of Advances in Modeling Earth Systems*, 11(2):485–513.

Koike, T., Kitao, M., Maruyama, Y., Mori, S., and Lei, T. T. (2001). Leaf morphology and photosynthetic adjustments among deciduous broad-leaved trees within the vertical canopy profile. *Tree Physiology*, 21(12-13):951–958.

Kunert, N., Aparecido, L. M. T., Wolff, S., Higuchi, N., Santos, J. d., Araujo, A. C. d., and Trumbore, S. (2017). A revised hydrological model for the Central Amazon: The importance of emergent canopy trees in the forest water budget. *Agricultural and Forest Meteorology*, 239:47–57.

Larjavaara, M. and Muller-Landau, H. C. (2013). Measuring tree height: a quantitative comparison of two common field methods in a moist tropical forest. *Methods in Ecology and Evolution*, 4(9):793–801.

Liu, H., Gleason, S. M., Hao, G., Hua, L., He, P., Goldstein, G., and Ye, Q. (2019). Hydraulic traits are coordinated with maximum plant height at the global scale. *Science Advances*, 5(2):eaav1332.

Liu, Y. and Muller, R. N. (1993). Effect of Drought and Frost on Radial Growth of Overstory and Undesrstory Stems in a Deciduous Forest. *The American Midland Naturalist*, 129(1):19–25.

Lloret, F., Keeling, E. G., and Sala, A. (2011). Components of tree resilience: effects of successive low-growth episodes in old ponderosa pine forests. *Oikos*, 120(12):1909–1920.

Martin-Benito, D. and Pederson, N. (2015). Convergence in drought stress, but a divergence of climatic drivers across a latitudinal gradient in a temperate broadleaf forest. *Journal of Biogeography*, 42(5):925–937.

Maréchaux, I., Bartlett, M. K., Sack, L., Baraloto, C., Engel, J., Joetzjer, E., and Chave, J. (2015). Drought tolerance as predicted by leaf water potential at turgor loss point varies strongly across species within an Amazonian forest. *Functional Ecology*, 29(10):1268–1277.

Maréchaux, I., Saint-André, L., Bartlett, M. K., Sack, L., and Chave, J. (2019). Leaf drought tolerance cannot be inferred from classic leaf traits in a tropical rainforest. *Journal of Ecology*.

Mazerolle, M. J. and portions of code contributed by Dan Linden. (2019). *AICcmodavg: Model Selection and Multimodel Inference Based on (Q)AIC(c)*. R package version 2.2-2.

McDowell, N. G. and Allen, C. D. (2015). Darcy's law predicts widespread forest mortality under climate warming. *Nature Climate Change*, 5(7):669–672.

McDowell, N. G., Bond, B. J., Dickman, L. T., Ryan, M. G., and Whitehead, D. (2011). Relationships Between Tree Height and Carbon Isotope Discrimination. In Meinzer, F. C., Lachenbruch, B., and Dawson, T. E., editors, *Size- and Age-Related Changes in Tree Structure and Function*, Tree Physiology, pages 255–286. Springer Netherlands, Dordrecht.

Meakem, V., Tepley, A. J., Gonzalez-Akre, E. B., Herrmann, V., Muller-Landau, H. C., Wright, S. J., Hubbell, S. P., Condit, R., and Anderson-Teixeira, K. J. (2018). Role of tree size in moist tropical forest carbon cycling and water deficit responses. *New Phytologist*, 219(3):947–958.

Medeiros, C. D., Scoffoni, C., John, G. P., Bartlett, M. K., Inman-Narahari, F., Ostertag, R., Cordell, S., Giardina, C., and Sack, L. (2019). An extensive suite of functional traits distinguishes Hawaiian wet and dry forests and enables prediction of species vital rates. *Functional Ecology*, 33(4):712–734.

Metcalfe, P., Beven, K., and Freer, J. (2018). *dynatopmodel: Implementation of the Dynamic TOPMODEL Hydrological Model*. R package version 1.2.1.

Muller-Landau, H. C., Condit, R. S., Chave, J., Thomas, S. C., Bohlman, S. A., Bunyavejchewin, S., Davies, S., Foster, R., Gunatilleke, S., Gunatilleke, N., Harms, K. E., Hart, T., Hubbell, S. P., Itoh, A., Kassim, A. R., LaFrankie, J. V., Lee, H. S., Losos, E., Makana, J.-R., Ohkubo, T., Sukumar, R., Sun, I.-F., Nur Supardi, M. N., Tan, S., Thompson, J., Valencia, R., Muñoz, G. V., Wills, C., Yamakura, T., Chuyong, G., Dattaraja, H. S., Esufali, S., Hall, P., Hernandez, C., Kenfack, D., Kiratiprayoon, S., Suresh, H. S., Thomas, D., Vallejo, M. I., and Ashton, P. (2006). Testing metabolic ecology theory for allometric scaling of tree size, growth and mortality in tropical forests. *Ecology Letters*, 9(5):575–588.

NEON (2018). National Ecological Observatory Network. 2016, 2017, 2018. Data Products: DP1.00001.001, DP1.00098.001, DP1.00002.001. Provisional data downloaded from http://data.neonscience.org/ in May 2019. Battelle, Boulder, CO, USA.

Olson, M. E., Soriano, D., Rosell, J. A., Anfodillo, T., Donoghue, M. J., Edwards, E. J., León-Gómez, C., Dawson, T., Martínez, J. J. C., Castorena, M., Echeverría, A., Espinosa, C. I., Fajardo, A., Gazol, A., Isnard, S., Lima, R. S., Marcati, C. R., and Méndez-Alonzo, R. (2018). Plant height and hydraulic vulnerability to drought and cold. *Proceedings of the National Academy of Sciences*, 115(29):7551–7556.

Powell, T. L., Wheeler, J. K., Oliveira, A. A. R. d., Costa, A. C. L. d., Saleska, S. R., Meir, P., and Moorcroft, P. R. (2017). Differences in xylem and leaf hydraulic traits explain differences in drought tolerance among mature Amazon rainforest trees. *Global Change Biology*, 23(10):4280–4293.

Pretzsch, H., Schütze, G., and Biber, P. (2018). Drought can favour the growth of small in relation to tall trees in mature stands of Norway spruce and European beech. *Forest Ecosystems*, 5(1):20.

R Core Team (2019). *R: A Language and Environment for Statistical Computing*. R Foundation for Statistical Computing, Vienna, Austria.

Rodríguez-Catón, M., Villalba, R., Srur, A. M., and Luckman, B. (2015). Long-term trends in radial growth associated with Nothofagus pumilio forest decline in Patagonia: Integrating local- into regional-scale patterns. *Forest Ecology and Management*, 339:44–56.

Rosas, T., Mencuccini, M., Barba, J., Cochard, H., Saura-Mas, S., and Martínez-Vilalta, J. (2019). Adjustments and coordination of hydraulic, leaf and stem traits along a water availability gradient. *New Phytologist*, 223(2):632–646.

Roskilly, B., Keeling, E., Hood, S., Giuggiola, A., and Sala, A. (2019). Conflicting functional effects of xylem pit structure relate to the growth-longevity trade-off in a conifer species. *PNAS. doi: /10.1073/pnas.1900734116.*

Ryan, M. G., Phillips, N., and Bond, B. J. (2006). The hydraulic limitation hypothesis revisited. *Plant, Cell & Environment*, 29(3):367–381.

Sapes, G., Roskilly, B., Dobrowski, S., Maneta, M., Anderegg, W. R. L., Martinez-Vilalta, J., and Sala, A. (2019). Plant water content integrates hydraulics and carbon depletion to predict drought-induced seedling mortality. *Tree Physiology*, 39(8):1300–1312.

Scharnweber, T., Heinze, L., Cruz-García, R., van der Maaten-Theunissen, M., and Wilmking, M. (2019). Confessions of solitary oaks: We grow fast but we fear the drought. *Dendrochronologia*, 55:43–49.

Schöngart, J., Bräuning, A., Barbosa, A. C. M. C., Lisi, C. S., and de Oliveira, J. M. (2017). Dendroecological Studies in the Neotropics: History, Status and Future Challenges. In Amoroso, M. M., Daniels, L. D., Baker, P. J., and Camarero, J. J., editors, *Dendroecology: Tree-Ring Analyses Applied to Ecological Studies*, Ecological Studies, pages 35–73. Springer International Publishing, Cham.

Scoffoni, C., Vuong, C., Diep, S., Cochard, H., and Sack, L. (2014). Leaf Shrinkage with Dehydration: Coordination with Hydraulic Vulnerability and Drought Tolerance. *Plant Physiology*, 164(4):1772–1788.

Simeone, C., Maneta, M. P., Holden, Z. A., Sapes, G., Sala, A., and Dobrowski, S. Z. (2019). Coupled ecohydrology and plant hydraulics modeling predicts ponderosa pine seedling mortality and lower treeline in the US Northern Rocky Mountains. *New Phytologist*, 221(4):1814–1830.

Slette, I. J., Post, A. K., Awad, M., Even, T., Punzalan, A., Williams, S., Smith, M. D., and Knapp, A. K. (2019). How ecologists define drought, and why we should do better. *Global Change Biology*, 0(0):1–8.

Smith, W. K. and Nobel, P. S. (1977). Temperature and Water Relations for Sun and Shade Leaves of a Desert Broadleaf, Hyptis emoryi. *Journal of Experimental Botany*, 28(1):169–183.

Sohn, J. A., Saha, S., and Bauhus, J. (2016). Potential of forest thinning to mitigate drought stress: A meta-analysis. *Forest Ecology and Management*, 380:261–273.

Stovall, A. E. L., Anderson-Teixeira, K. J., and Shugart, H. H. (2018a). Assessing terrestrial laser scanning for developing non-destructive biomass allometry. *Forest Ecology and Management*, 427:217–229.

Stovall, A. E. L., Anderson-Teixeira, K. J., and Shugart, H. H. (2018b). Terrestrial LiDAR-derived non-destructive woody biomass estimates for 10 hardwood species in Virginia. *Data in Brief*, 19:1560–1569.

Stovall, A. E. L., Shugart, H., and Yang, X. (2019). Tree height explains mortality risk during an intense drought. *Nature Communications*, 10(1):1–6.

Suarez, M. L., Ghermandi, L., and Kitzberger, T. (2004). Factors predisposing episodic drought-induced tree mortality in Nothofagus– site, climatic sensitivity and growth trends. *Journal of Ecology*, 92(6):954–966.

Sørensen, R., Zinko, U., and Seibert, J. (2006). On the calculation of the topographic wetness index: evaluation of different methods based on field observations. *Hydrology and Earth System Sciences*, 10(1):101–112.

Trenberth, K. E., Dai, A., van der Schrier, G., Jones, P. D., Barichivich, J., Briffa, K. R., and Sheffield, J. (2014). Global warming and changes in drought. *Nature Climate Change*, 4(1):17–22.

Twery, M. J. (1991). Effects of defoliation by gypsy moth. *IN: Gottschalk, Kurt W.; Twery, Mark J.; Smith, Shirley I., eds. Proceedings, U.S. Department of Agriculture interagency gypsy moth research review 1990; East Windsor, CT. Gen. Tech. Rep. NE-146. Radnor, PA: U.S. Department of Agriculture, Forest Service, Northeastern Forest Experiment Station. 27-39.*, 146.

van der Maaten-Theunissen, M. and van der Maaten, E. (2016). *pointRes: Analyzing Pointer Years and Components of Resilience*. R package version 1.1.3.

Zuleta, D., Duque, A., Cardenas, D., Muller-Landau, H. C., and Davies, S. J. (2017). Drought-induced mortality patterns and rapid biomass recovery in a terra firme forest in the Colombian Amazon. *Ecology*, 98(10):2538–2546.

Table 1. Summary of hypotheses, corresponding specific predictions, and results. We count predictions as fully supported ('yes') when the response is signficant in single-variable tests (Table 4) and included in all top full models and as partially supported ('(yes)') or rejected ('(no)') when the direction of response consistently matched the prediction but the effect was not significant in all models.

	Prediction supported?				
Hypotheses & Specific Predictions	Overall	1966	1977	1999	Results
Tree size and microenvironment					
Larger, taller trees have lower Rt.					
Rt decreases with stem diameter (DBH).	yes	yes	-	-	Table 4
Rt decreases with height (H).	yes	yes	-	(yes)	Tables 4, 5
Trees with more exposed crowns have lower Rt.					
Dominant trees have lowest Rt.	-	yes	(yes)	-	Tables 4, 5
Correcting for H, dominant trees have lowest Rt.	(no)		-	(no)	Tables 4, 5
Small trees (lower root volume) in drier microhabitats have lower Rt.					
There is a negative interactive effect between H and topographic wetness index.	-	-	-	-	Table 4
Species traits					
Species' traits–particularly leaf hydraulic traits–predict Rt.					
Wood density correlates (positively or negatively) to Rt.	-	-	-	-	Table 4
Leaf mass per area correlates positively to Rt.	-	-	-	-	Table 4
Ring-porous species have higher Rt than diffuse- or semi-ring- porous.	-	yes	(no)	yes	Tables 4, 5
Percent loss leaf area upon desiccation correlates negatively with Rt.	yes	yes	(yes)	-	Tables 4, 5
Water potential at turgor loss correlates negatively with Rt.	(yes)	-	(yes)	(yes)	Tables 4, 5

Table 2. Summary of variables.

variable	symbol	units	description	category	n
Dependent variable					
drought resistance	Rt	-	ratio of growth during drought year to mean growth of the 5 years prior.	-	1596
Independent variables					
drought year	Y	-	year of drought	1966	478
				1977	547
				1999	571
tree size					
diameter breast height	DBH	cm	DBH in drought year	-	all
height	H	m	estimated H in drought year	-	all
microhabitat					
crown position		-	2018 crown position	dominant (D)	31
				co-dominant (C)	231
				intermediate (I)	224
				suppressed (S)	101
topographic wetness index	TWI	-	steady-state wetness index based on slope and upstream contributing area	-	all
species' traits					
wood density	WD	g cm^{-3}	dry mass of a unit volume of fresh wood	-	all
leaf mass per area	LMA	kg m^{-2}	ratio of leaf dry mass to fresh leaf area	-	all
xylem porosity		-	vessel arrangement in xylem	ring (R)	408
				semi-ring (SR)	31
				diffuse (D)	178
turgor loss point	π_{tlp}	MPa	water potential at which leaves wilt	-	all
percent loss area	PLA_{dry}	%	percent loss of leaf area upon dessication	-	all

Table 3. Overview of analyzed species, listed in order of their relative contributions to woody stem productivity ($ANPP_{stem}$) in the plot, along with numbers and sizes sampled, and species traits. Variable abbreviations are as in Table 2.

			DBH (cm)		species traits (mean +/- sd)				
species	$\%\, ANPP_{stem}$	n cores	mean	range	WD ($g\,cm^{-3}$)	LMA ($g\,cm^{-2}$)	xylem porosity	π_{tlp} (Mpa)	PLA (%)
Liriodendron tulipifera (LITU)	47.1	98	368.54	100 - 1004	0.4 ± 0.03	46.92 ± 12.38	diffuse	-1.92 ± 0.17	19.56 ± 2.06
Quercus alba (QUAL)	10.7	61	471.51	114 - 791	0.61 ± 0.02	75.8 ± 11.05	ring	-2.58 ± 0.08	8.52 ± 0.37
Quercus rubra (QURU)	10.1	69	548.79	110.7 - 1480	0.62 ± 0.02	71.13 ± 6.70	ring	-2.64 ± 0.28	11.01 ± 0.84
Quercus velutina (QUVE)	7.8	77	541.38	160.2 - 1142	0.65 ± 0.04	48.69 ± 3.30	ring	-2.39 ± 0.15	13.42 ± 0.84
Quercus montana (QUPR)	4.8	59	422.48	105 - 872	0.61 ± 0.01	71.77 ± 40.17	ring	-2.36 ± 0.09	11.75 ± 1.37
Fraxinus americana (FRAM)	3.8	62	353.63	64 - 947.3	0.56 ± 0.01	43.28 ± 4.78	ring	-2.1 ± 0.36	13.06 ± 1.06
Carya glabra (CAGL)	3.7	31	313.89	98 - 985	0.62 ± 0.04	42.76 ± 0.94	ring	-2.13 ± 0.50	21.09 ± 5.48
Juglans nigra (JUNI)	2.1	31	481.42	242 - 870	1.09 ± 0.09	72.13 ± 7.10	semi-ring*	-2.76 ± 0.21	24.64 ± 8.72
Carya cordiformis (CACO)	2.0	13	271.87	107 - 615	0.83 ± 0.10	45.86 ± 15.60	ring	-2.13 ± 0.45	17.22 ± 2.25
Carya tomentosa (CATO)	2.0	13	209.74	121 - 322.1	0.83	45.36	ring	-2.2	16.56
Fagus grandifolia (FAGR)	1.5	80	235.11	112 - 1072	0.62 ± 0.03	30.68 ± 4.94	diffuse	-2.57	9.45 ± 1.25
Carya ovalis (CAOVL)	1.1	23	352.87	149 - 660	0.96 ± 0.33	47.6 ± 3.95	ring	-2.48 ± 0.04	14.8 ± 6.34

* Semi-ring porosity is intermediate between ring and diffuse. We group it with diffuse-porous species for more even division of species between categories.

Table 4. Single-variable tests of hypothesized drivers of drought resistance. Models including each variable were compared to corresponding null models. dAIC is the AICc of the null model minus that of the model including the variable (thus, dAICc>2 indicates that the variable significantly improves the model). Variable abbreviations are as in Table 2.

			all droughts		1966		1977		1999	
variable	category	null model variables	dAICc	coefficients	dAICc	coefficients	dAICc	coefficients	dAICc	coefficients
Tree size and microenvironment										
ln[DBH]		(year)	8.17**	-0.0385	15.32**	-0.0888	-0.87	-0.0214	-1.93	0.0057
ln[H]		(year)	8.17**	-0.0600	15.32**	-0.1383	-0.87	-0.0334	-1.93	0.0089
crown position	D	(year)	-2.96	-0.0461	3.25**	-0.0509	0.66	-0.0759	0.38	-0.0103
(alone)	C		-	0.0000	-	0.0000	-	0.0000	-	0.0000
	I		-	-0.0063	-	0.0732	-	-0.0298	-	-0.0563
	S		-	0.0122	-	0.0526	-	0.0432	-	-0.0483
crown position	D	ln[H] (+year)	0.57	-0.0347	-1.84	-0.0328	-0.23	-0.0730	3.04**	-0.0024
(with height)	C		-	0.0000	-	0.0000	-	0.0000	-	0.0000
	I		-	-0.0425	-	0.0139	-	-0.0388	-	-0.0810
	S		-	-0.0582	-	-0.0662	-	0.0258	-	-0.0956
ln[TWI]		ln[H] (+year)	5.34**	-0.0890	-1.96	-0.0171	5.05**	-0.1404	2.8**	-0.1033
ln[TWI]*ln[H]		ln[H]+ln[TWI] (+year)	-0.83	0.0797	-1.58	0.0927	-1.47	0.0861	-1.9	0.0414
Species traits										
WD		ln[H] (+year)	-1.91	-0.0479	-1.24	-0.2089	-1.22	-0.1812	0.22	0.2502
LMA		ln[H] (+year)	-1.99	0.0003	-1.88	0.0012	-1.76	-0.0013	-2	0.0004
xylem porosity	R	ln[H] (+year)	-0.71	0.0660	2.305**	0.1888	1.399*	-0.1452	3.765**	0.1544
	D/SR		-	0.0000	-	0.0000	-	0.0000	-	0.0000
π_{tlp}		ln[H] (+year)	1.33*	-0.1777	-1.64	-0.1078	1.26*	-0.2500	0.016	-0.1732
PLA		ln[H] (+year)	7.17**	-0.0140	9.18**	-0.0249	-0.05	-0.0105	-0.716	-0.0074

*dAICc > 1: variable qualified for inclusion in full model

**dAICc > 2: statistically signficant, variable qualified for inclusion in full model

Table 5. Summary of top full models for each drought instance. Models are ranked by AICc, and we show all models whose AICc value falls within 1.0 (dAICc<1) of the best model (bold).

					crown position					xylem porosity			
drought	dAICc	R^2	Intercept	$ln[H]$	D	C	I	S	$ln[TWI]$	D/SR	R	PLA	π_{tlp}
all	**0.000**	**0.12**	**1.077**	**-0.057**	**-**	**-**	**-**	**-**	**-0.086**	**-**	**-**	**-0.012**	**-0.113**
	0.586	0.11	1.365	-0.055	-	-	-	-	-0.086	-	-	-0.013	-
	0.726	0.12	1.220	-0.089	-0.034	0	-0.037	-0.051	-0.079	-	-	-0.012	-0.101
	0.813	0.11	1.481	-0.089	-0.034	0	-0.039	-0.054	-0.079	-	-	-0.014	-
1966	**0.000**	**0.25**	**1.503**	**-0.141**	**-**	**-**	**-**	**-**	**-**	**0**	**0.11**	**-0.021**	**-**
1977	**0.000**	**0.21**	**1.136**	**-**	**-**	**-**	**-**	**-**	**-0.145**	**0**	**-0.205**	**-0.015**	**-0.13**
	0.040	0.21	1.490	-	-	-	-	-	-0.145	0	-0.22	-0.017	-
	0.505	0.22	1.089	-	-0.069	0	-0.025	0.043	-0.137	0	-0.199	-0.014	-0.143
	0.818	0.22	1.481	-	-0.07	0	-0.027	0.038	-0.136	0	-0.216	-0.017	-
1999	**0.000**	**0.23**	**0.464**	**-**	**-**	**-**	**-**	**-**	**-0.095**	**0**	**0.16**	**-**	**-0.197**
	0.019	0.24	0.725	-0.068	0	0	-0.077	-0.09	-0.084	0	0.167	-	-0.183

Figure Legends

Figure 1. Climate and species-level growth responses over our study period, highlighting the three focal drougths (a) and community-wide responses Time series plot (**a**) shows peak growing season (May-August) climate conditions and residual chronologies for each species. PET and PRE data were obtained from the Climatic Research Unit high-resolution gridded dataset (CRU TS v.4.01; Harris et al. 2014). Focal droughts are indicated by dashed lines, and shading indicates the pre-drought period used in calculations of the resistance metric. Figure modified from Helcoski *et al.* (2019). Density plots (**b**) show the distribution of resistance values for each drought.

Figure 2. Height profiles in growing season climatic conditions, tree heights by crown position, and leaf hydraulic traits Shown are averages (± SD) of daily maxima and minima of (**a**) wind speed, (**b**) relative humidity (RH), and (**c**) air temperature (T_{air}) averaged over each month of the peak growing season (May-August) from 2016-2018. In these plots, heights are slightly offset for visualization purposes. Also shown is (**d**) 2018 tree heights by canopy position (see Table 2 for codes). In all plots, the dashed horizontal line indicates the 95th percentile of tree heigts in the ForestGEO plot.

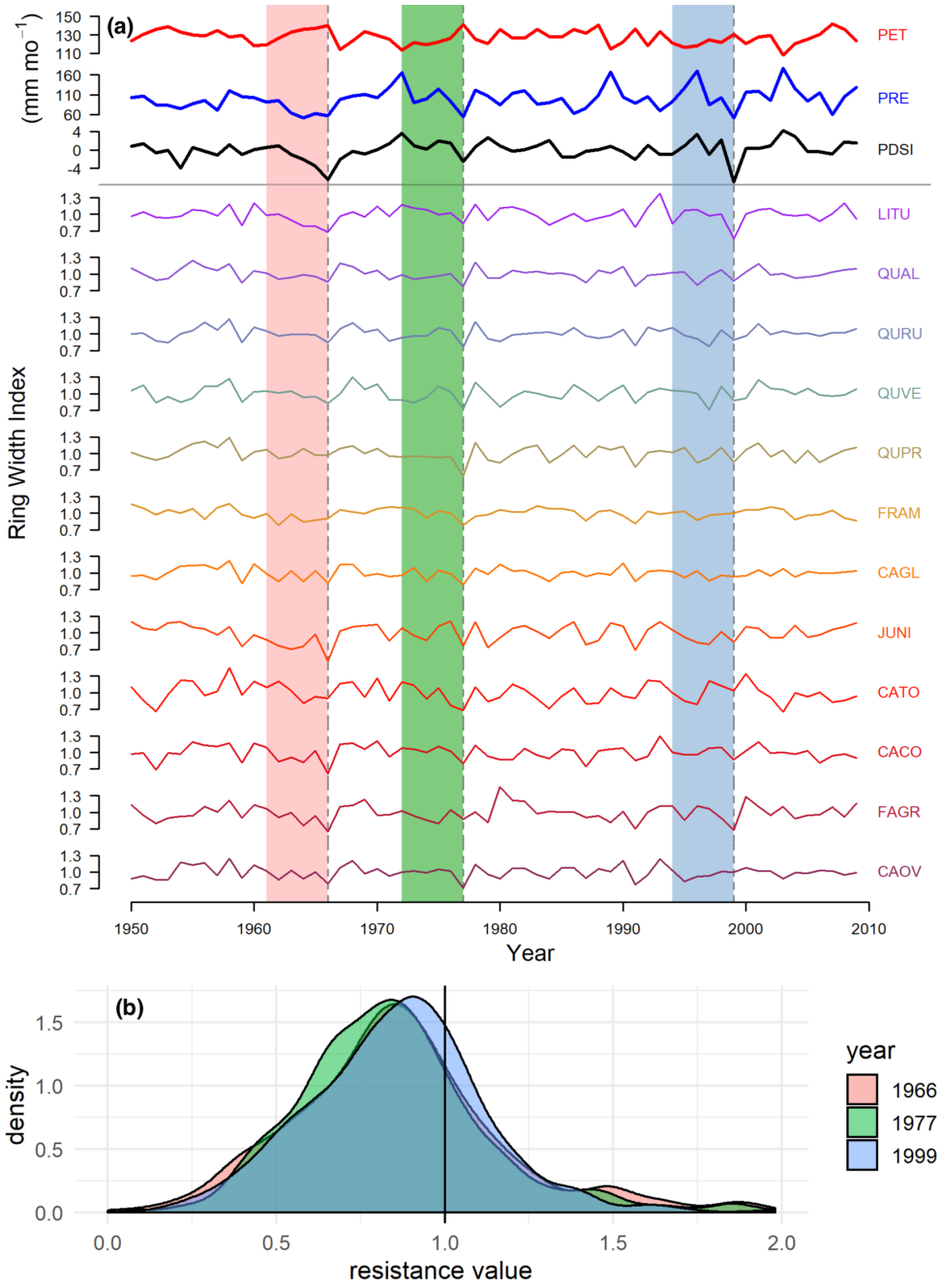

Figure 1. Climate and species-level growth responses over our study period, highlighting the three focal drougths (a) and community-wide responses Time series plot (a) shows peak growing season (May-August) climate conditions and residual chronologies for each species. PET and PRE data were obtained from the Climatic Research Unit high-resolution gridded dataset (CRU TS v.4.01; Harris et al. 2014). Focal droughts are indicated by dashed lines, and shading indicates the pre-drought period used in calculations of the resistance metric. Figure modified from Helcoski *et al.* (2019). Density plots (b) show the distribution of resistance values for each drought.

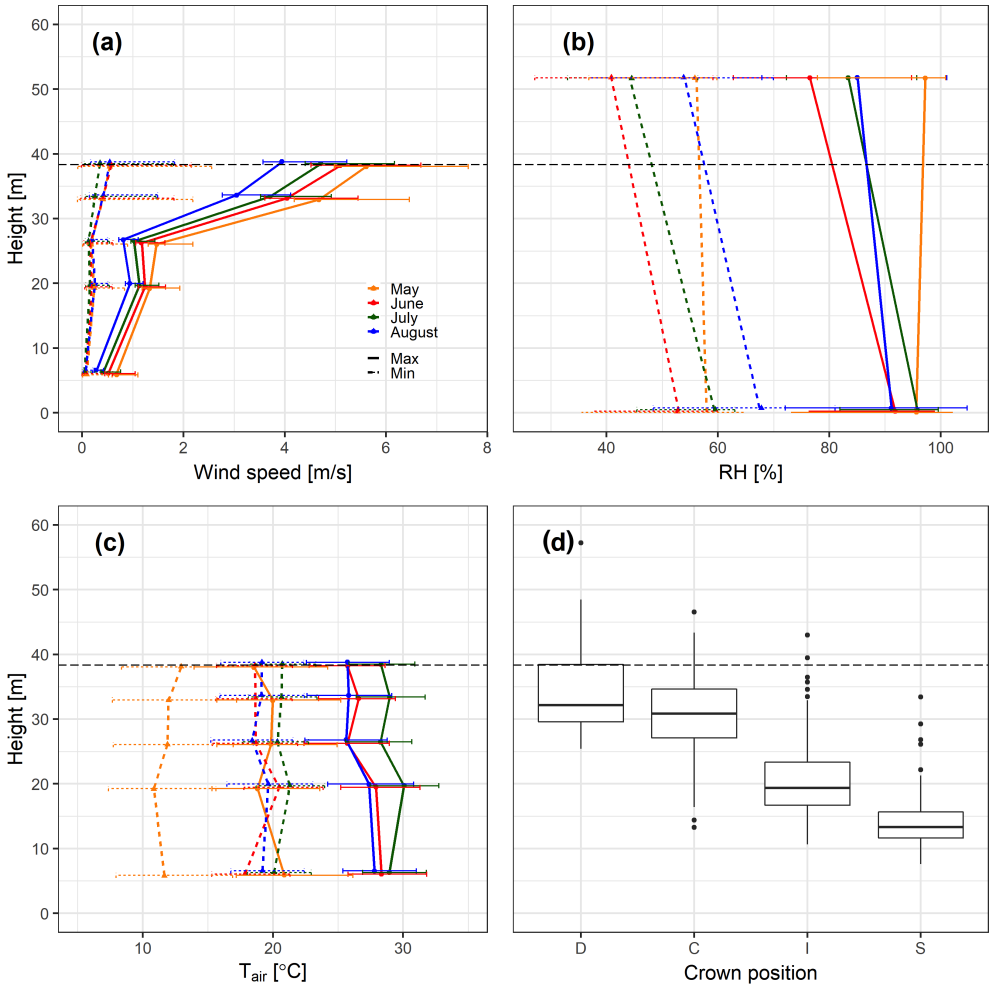

Figure 2. Height profiles in growing season climatic conditions, tree heights by crown position, and leaf hydraulic traits The top row shows averages (± SD) of daily maxima and minima of (a) wind speed, (b) relative humidity (RH), and (c) air temperature (T_{air}) averaged over each month of the peak growing season (May-August) from 2016-2018. In these plots, heights are slightly offset for visualization purposes. Also shown is (d) 2018 tree heights by canopy position (see Table 2 for codes). In all plots, the dashed horizontal line indicates the 95th percentile of tree heigts in the ForestGEO plot.